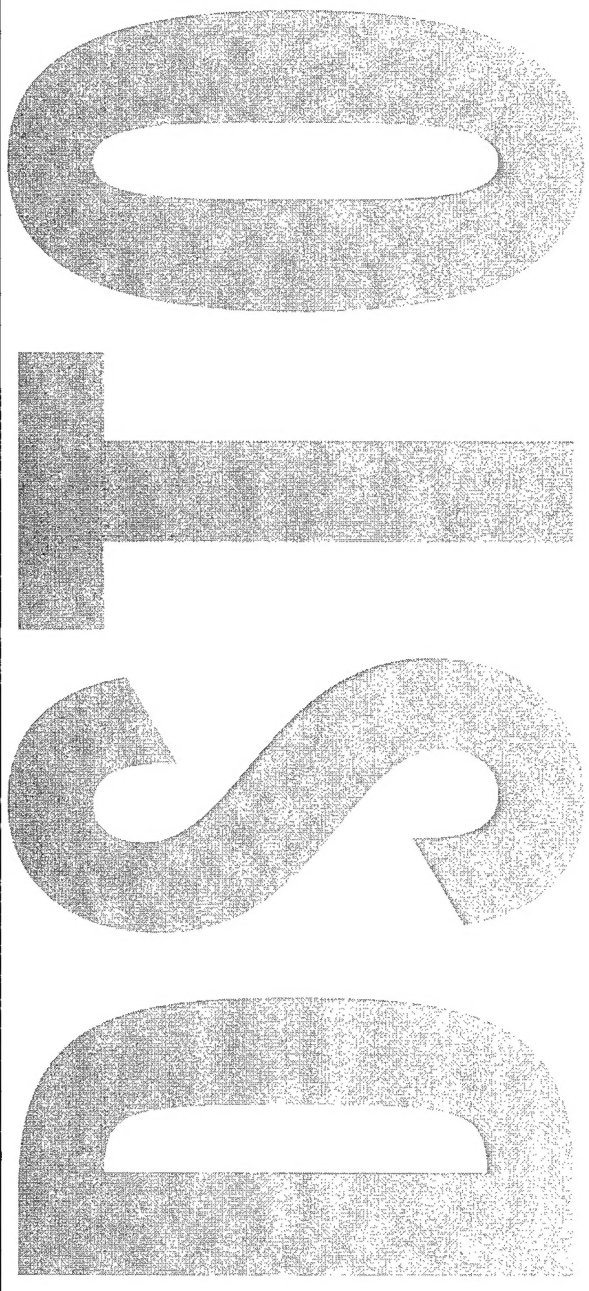

The Effect of Non-spherical Collapse on Determination of Explosion Bubble Parameters

John P. Best

DSTO-RR-0238

DEFENCE
SCIENCE & TECHNOLOGY

The Effect of Non-spherical Collapse on Determination of Explosion Bubble Parameters

John P. Best

Maritime Operations Division
Systems Sciences Laboratory

DSTO–RR–0238

ABSTRACT

The technique developed by Arons (1948) for determining the parameters that characterise the adiabatic model of underwater explosion bubble contents is revised to account for the effect of non-spherical collapse. Additional modifications are made to enhance accuracy. The parameters predicted are similar to those given by Arons but consideration of the pressure in the fluid when the bubble rebounds shows the agreement to be somewhat fortuitous. Error bounds for the parameters are given for the first time.

Published by

DSTO Systems Sciences Laboratory
PO Box 1500
Edinburgh, South Australia, Australia 5111

Telephone: (08) 8259 5555
Facsimile: (08) 8259 6567

AR-012-368
July, 2002

APPROVED FOR PUBLIC RELEASE

The Effect of Non-spherical Collapse on Determination of Explosion Bubble Parameters

EXECUTIVE SUMMARY

Over recent years there has been considerable interest in the behaviour of the bubble formed when a mass of explosive is detonated underwater. Of specific concern is the behaviour of the bubble upon collapse, when a high speed liquid jet is formed, generally in a direction towards nearby structures. Although it is possible to predict the shape of bubbles as they collapse, no decisive computational capability has been demonstrated for predicting the loads experienced by a target due to nearby explosion bubble collapse. Attempts are underway to utilise boundary integral methods to predict target loadings.

A key challenge in application of the boundary integral method is to determine the parameters that describe the gaseous bubble contents in terms of the mass and type of explosive, and the depth at which it is detonated. It is typically assumed that a quantity of ideal gas is contained within the bubble and undergoes adiabatic expansions and contractions as the bubble oscillates. Such a model is characterised by the bubble energy per mass of explosive, denoted by ϵ, the ratio of specific heats, γ, and a constant, κ, that defines the adiabatic along which the gas expands and contacts.

Methodologies for determining these three parameters are generally based upon measurements of key physical quantities associated with the bubble oscillation, with the contribution of Arons[1] essential in this regard. Arons embarked upon a determination of ϵ, γ and κ by assuming the bubble remains spherical throughout the first oscillation period. This assumption allows analytical expressions to be obtained for the period and peak pressure caused by the first bubble rebound. The three parameters are determined so that spherical bubble model predictions are in close agreement with measurements of period and peak pressure at rebound.

Investigations of recent years have made it clear that the assumption the bubble remains spherical throughout its motion is adequate during the growth and early collapse phases, but fails as the bubble approaches minimum volume and rebounds. Experimental and theoretical studies have shown the formation of a high speed liquid jet upon collapse, which travels through the bubble and causes it to evolve into toroidal form. For deep detonations the jet is directed upwards owing to the action of buoyancy.

The principal contribution of this report is to modify the technique of Arons to account for the effect that deformation from spherical shape has upon the pressure field and associated determination of ϵ, γ and κ. Error bounds for these parameters are also given for the first time. Having determined ϵ, γ and κ, the variation of peak pressure at bubble minimum with charge mass, distance from the charge and depth is investigated. The behaviour is considerably different from that predicted using the spherical bubble model and is interpreted in terms of the non-spherical collapse behaviour of the bubble. In view of the complex behaviour shown, it appears to be somewhat fortuitous that Arons obtained good estimates of the three parameters on the basis of the spherical bubble model.

[1] *J. Acoust. Soc. Am.*, **20**, 277-282, 1948.

Author

John P. Best
Maritime Operations Division

John Best is a Principal Research Scientist in Maritime Operations Division. He holds a Bachelor of Science degree with First Class Honours in Physics from the University of Queensland, and a PhD in Applied Mathematics from the University of Wollongong. His early research was concerned with development of theoretical and numerical methods for predicting underwater weapon effects. Later research in support of minewarfare operations included sonar modelling, analysis of novel tactics and human factors. More recently he initiated DSTO's Virtual Ship project, leading development of the underlying simulation architecture. In his current role of Head Surface Ship Combat Systems, he leads a group that undertakes analysis in support of combat system acquisition, development and support. A principal component of the group's effort is use of synthetic environments to enable human-in-the-loop experimentation.

Contents

1 Introduction

Over recent years there has been considerable interest in the behaviour of the bubble formed when a mass of explosive is detonated underwater. Of specific concern is the behaviour of the bubble upon collapse, when a high speed liquid jet is formed, generally in a direction towards nearby structures. Although it is possible to predict the shape of bubbles as they collapse, no decisive computational capability has been demonstrated for predicting the loads experienced by a target due to nearby explosion bubble collapse. Attempts are underway, however, to utilise boundary integral methods to predict target loadings.

This report concerns the various parameters that characterise the boundary integral calculation, and these are introduced in section 3. The key challenge is to determine these parameters in terms of the mass and type of explosive, and the depth at which it is detonated. The problem revolves around the mathematical description of the gaseous bubble contents. It is typically assumed that a quantity of ideal gas is contained within the bubble and undergoes adiabatic expansions and contractions as the bubble oscillates. Such a model is characterised by the bubble energy per mass of explosive, denoted by ϵ, the ratio of specific heats, γ, and the constant that defines the adiabatic along which the gas expands and contacts. This constant κ is such that

$$p\rho^{-\gamma} = \kappa, \tag{1}$$

where p and ρ are respectively the explosion bubble gas pressure and density.

Methodologies for determining these three parameters are generally based upon measurements of key physical quantities associated with the bubble oscillation. In particular, experimental data for the first bubble period, T, and maximum bubble radius, R_m, are commonly available for the explosive TNT. Data for the peak pressure at some point in the flow field as the bubble rebounds for the first time are also commonly available. Arons, Slifko & Carter (1948) presented such data for TNT.

In the context of this report the contribution of Arons (1948) is essential. Arons embarked upon a determination of ϵ, γ and κ by assuming the bubble remains spherical throughout the first oscillation period. This assumption allows analytical expressions to be obtained for the period and peak pressure caused by the first bubble rebound. The three parameters are determined so that spherical bubble model predictions are in close agreement with measurements of period and peak pressure at rebound.

Investigations of recent years have made clear that the assumption the bubble remains spherical throughout the motion is adequate during the growth and early collapse phase, but fails as the bubble approaches minimum volume and rebounds. Experimental and theoretical studies (Benjamin & Ellis 1966, Lauterborn & Bolle 1975, Tomita & Shima 1986, Blake & Gibson 1987, Vogel, Lauterborn & Timm 1989, Plesset & Chapman 1971, Guerri, Lucca & Prosperetti 1981, Blake, Taib & Doherty 1986, Chahine & Perdue 1988, Wilkerson 1989, Best & Kucera 1992, Best 1993, Szymczak, Rogers, Solomon & Berger 1993) have shown the formation of a high speed liquid jet upon collapse, which travels through the bubble and causes it to evolve into toroidal form. For deep detonations the jet is directed upwards owing to the action of buoyancy. It has also been shown that under some circumstances the jet does not completely penetrate the bubble before minimum

volume is achieved (Best & Kucera 1992). In these cases the jet continues to travel through the bubble as it re-expands.

The principle contribution of this report is to modify the technique of Arons (1948) to account for the effect that deformation from spherical shape has upon the pressure field and associated determination of the three parameters γ, ϵ and κ that characterise the bubble contents. The technique is further modified so that the parameters yield predictions of bubble period that differ from the experimental data over the range of their validity by the minimum amount, in a least squares sense.

In section 2 the experimental data essential to this report are reviewed. The boundary integral method for bubbles is reviewed in section 3 and in section 4 the spherical bubble model is presented and the non-dimensional parameters that characterise the boundary integral calculation are derived in terms of γ, ϵ and κ. In section 5 the methodology for determining γ, ϵ and κ using a boundary integral method is described. By imposing that the theoretical bubble period differs from experimental data by a minimal amount, in a least squares sense, the parameters γ and ϵ are obtained. The pressure data of Arons *et al.* (1948) are then used to fix κ. As κ is varied the boundary integral method is used to compute the pressure in the flow at the point corresponding to Arons *et al.*'s measurements. κ is varied until agreement is achieved with the peak pressure at bubble minimum. Error bounds on γ, ϵ and κ are computed.

Having determined γ, ϵ and κ, the variation of peak pressure at bubble minimum with charge mass, distance from the charge and depth is investigated. The behaviour is considerably different from that predicted using the spherical bubble model and is interpreted in terms of the non-spherical collapse behaviour of the bubble. In view of the complex behaviour shown, it appears to be somewhat fortuitous that Arons obtained good estimates of γ, ϵ and particularly κ on the basis of the spherical bubble model.

2 Summary of essential experimental data

Data for the first period of oscillation and maximum radius of an explosion bubble have been compiled over a range of charge masses and depths of detonation. These data are summarized according to the following formulae:

$$T = K\frac{w^{1/3}}{(\xi+\xi_0)^{5/6}}, \tag{2}$$

$$R_m = J\Big(\frac{w}{\xi+\xi_0}\Big)^{1/3}. \tag{3}$$

In these expressions w is the charge mass in kilograms, ξ is the depth of the detonation in metres and ξ_0 is the atmospheric pressure in metres of water, also known as the atmospheric head. The constants K and J are given by Swift & Decius (1947) as

$$J = 3.36\,\mathrm{m}^{4/3}\mathrm{kg}^{-1/3}, \qquad K = 2.11\,\mathrm{s}\,\mathrm{m}^{5/6}\mathrm{kg}^{-1/3}.$$

It is pertinent to note that Swisdak (1978) quotes an identical value of K but utilises a value of $J = 3.50\,\mathrm{m}^{4/3}\mathrm{kg}^{-1/3}$. At the time these data were compiled charge mass was

typically measured in pounds, and distances given in feet. In these units the coefficients are (Swift & Decius 1947)

$$J = 12.6\,\mathrm{ft}^{4/3}\mathrm{lb}^{-1/3}, \qquad K = 4.36\,\mathrm{s\,ft}^{5/6}\mathrm{lb}^{-1/3},$$

with Swisdak giving $J = 13.1\,\mathrm{ft}^{4/3}\mathrm{lb}^{-1/3}$. According to Szymczak & Solomon (1996), Swisdak published a higher value for J following reappraisal of the data presented by Swift & Decius (1947).

The period data are central to the calculation here and since error bounds on the estimates of γ, ϵ and κ are required, an error estimate of the period coefficient K is necessary. The data presented by Swift & Decius (1947) give $K = 4.36 \pm 0.014\,\mathrm{s\,ft}^{5/6}\mathrm{lb}^{-1/3}$, where the error is the standard deviation of the mean. Converting to SI units and retaining three significant figures gives $K = 2.11 \pm 0.01\,\mathrm{s\,m}^{5/6}\mathrm{kg}^{-1/3}$.

Data for the peak pressure experienced in the fluid surrounding the bubble at about the time of rebound are central to this study, and the technique used by Arons (1948). Arons *et al.* (1948) presented such data for the pressure measured at a distance R_p from the charge that satisfied

$$R_p = w_{\mathrm{lb}}^{1/3}/0.352\,\mathrm{ft}, \qquad R_p = w^{1/3}/0.887\,\mathrm{m}, \tag{4}$$

where w_{lb} is the charge mass in pounds and w is the charge mass is in kilograms. The peak pressure was measured for charge masses 0.229 kg (0.505 lb) and 1.137 kg (2.507 lb) at depths of 76.2 m (250 ft) and 152.4 m (500 ft), and charges of mass 5.448 kg (12.01 lb) at a depth of 152.4 m (500 ft).

Arons *et al.* (1948) used cylindrical charges and measured the pressure at the distance R_p at positions perpendicular to the cylindrical surface, above, below and to the side of the charge. For the largest charge of 5.448 kg, a peak pressure over hydrostatic of $(7.860 \pm 0.069) \times 10^6$ Pa (1140 ± 10 lb/in^2) was recorded, with the error the standard deviation of the mean. Measurements were also made at a distance R_p from the charge along its axis. The complicating factor here was that the charge was detonated by a blasting cap at one end of the cylinder. For the 5.448 kg charge at a depth of 152.4 m, the peak over-pressures measured in this configuration were 8.274×10^6 Pa (1200 lb/in^2) at the end closest the blasting cap and 7.722×10^6 Pa (1120 lb/in^2) at the other end.

In the methodology described in this report it is intended to provide error bounds on the estimates of the parameters γ, ϵ and κ. A conservative approach is followed and the peak over-pressure at the first minimum for the 5.448 kg charge is taken to be $(7.929 \pm 0.345) \times 10^6$ Pa (1150 ± 50 lb/in^2). This range encompasses all the values quoted above. Note also that Arons (1948) used a value of 8.274×10^6 Pa (1200 lb/in^2) in his determination of the explosion bubble parameters.

For the main calculation presented here, the data for the 5.448 kg charge are used. In this case the problem of accounting for the mass of the detonator is minimised. For comparison, calculations have been performed using data for the 1.137 kg charge. The pressure measurements for the 0.229 kg charge show a much greater degree of scatter and hence are not used. Further, the objective of this report is to characterise the behaviour of larger quantities of explosive.

3 Review of the boundary integral method

Boundary integral methods are well suited to computing the motion of underwater explosion bubbles, from a time shortly after the detonation when the shock wave has travelled some distance from the bubble and the fluid may be considered incompressible. The strategy adopted in studies of underwater explosion bubble motion using the boundary integral method has been to assume that the bubble is initially spherical in shape and its surface at rest. A high initial pressure within the bubble drives the motion. Although these initial conditions are somewhat artificial, the key is to ensure that upon collapse the bubble rebounds at a volume very close to that at which rebound would occur in reality. Thus the initial conditions are chosen to ensure that this condition takes place. In the very early phases of the motion, just after the shock wave is transmitted into the water, buoyancy and the presence of nearby boundaries affect the bubble motion little. Hence any discrepancy between the real conditions and those used to commence boundary integral calculations are not expected to cause significant error in the predictions of bubble behaviour upon collapse, that being the aim of the exercise. It is further noted that Blake *et al.* (1986) demonstrated that the growth phase of a bubble may have a significant effect on the collapse behaviour and jet formation process. Hence it is essential that initial conditions are employed that permit calculation of most of the bubble expansion phase.

The boundary integral method follows from the assumption that the fluid is ideal and the flow induced by the bubble motion irrotational. A velocity potential ϕ is then introduced such that the fluid velocity is $\boldsymbol{u} = \nabla\phi$. For flow in a singly connected domain, the potential is written in the boundary integral form

$$c(\boldsymbol{p})\phi(\boldsymbol{p}) = \int_{\partial\Omega} \left(\frac{\partial\phi}{\partial n}(\boldsymbol{q}) G(\boldsymbol{p},\boldsymbol{q}) - \phi(\boldsymbol{q}) \frac{\partial G}{\partial n}(\boldsymbol{p},\boldsymbol{q}) \right) dS(\boldsymbol{q}), \tag{5}$$

with

$$c(\boldsymbol{p}) = \begin{cases} 2\pi & \boldsymbol{p} \in \partial\Omega, \\ 4\pi & \boldsymbol{p} \in \Omega \backslash \partial\Omega. \end{cases} \tag{6}$$

In these expressions $\boldsymbol{p}$ is the position vector of some point in the flow field, G is the Green's function, Ω the flow domain and $\partial\Omega$ its boundary. The normal to $\partial\Omega$ is $\boldsymbol{n}$, directed exterior to Ω, and $\partial/\partial n$ is the normal derivative. In problems of bubble dynamics, ϕ is typically known on free surfaces, including the bubble surface, $\partial\phi/\partial n$ is known on rigid boundaries and a solution of (5) is sought. Of particular relevance to the bubble is solution for the normal fluid velocity $\partial\phi/\partial n$ at its boundary.

The Bernoulli equation is

$$\frac{\partial\phi}{\partial t} + \frac{1}{2}|\nabla\phi|^2 + p_w/\rho_w + g(z-\xi) = p_\infty/\rho_w, \tag{7}$$

where p_w and ρ_w are the pressure and density of the water and g is the gravitational acceleration. The hydrostatic pressure at the depth ξ at which detonation occurs is p_∞, given by

$$p_\infty = p_a + \rho_w g\xi = \rho_w g(\xi_0 + \xi), \tag{8}$$

where the atmospheric pressure $p_a = \rho_w g\xi_0$. The Bernoulli equation allows $\partial\phi/\partial t$ to be eliminated from the equation

$$d\phi/dt = \partial\phi/\partial t + |\nabla\phi|^2, \tag{9}$$

which gives the rate of change of ϕ following a fluid element. Suppose the pressure within the bubble is specified independently of the details of the flow field. Then if (7) is evaluated at the bubble surface, p_w is known and (9) may be integrated in time to determine the evolution of ϕ at the bubble surface. Simultaneous integration of the equation

$$d\boldsymbol{X}/dt = \boldsymbol{u}, \tag{10}$$

describing the evolution of free surface particles in the Lagrangian sense, allows the motion of the surface to be computed in time. In (10) $\boldsymbol{X}$ is the position vector of a point on the bubble surface and $\boldsymbol{u}$ is the fluid velocity there. The Cartesian components of the fluid velocity at the bubble surface are obtained from the normal fluid velocity component, $\partial\phi/\partial n$, and the tangential component, obtained from knowledge of ϕ over the bubble. In accordance with (1), the pressure p within the bubble is

$$p = p_0(V_0/V)^\gamma, \tag{11}$$

where V is the volume, V_0 is its initial value and p_0 is the initial value of the pressure that drives the bubble motion from rest.

To bring out the key parameters that characterise the boundary integral approach, as introduced by Blake *et al.* (1986) and later Best & Kucera (1992), the formulation is transformed to dimensionless variables. The distance scale is R_m, the maximum radius to which the bubble would expand if it remained spherical, the time scale is $R_m(\rho_w/p_\infty)^{1/2}$ and the pressure scale is p_∞. Denoting dimensionless quantities by $'$, the Bernoulli equation becomes

$$\frac{\partial\phi'}{\partial t'} + \frac{1}{2}|\nabla\phi'|^2 + \alpha(V'/V_0')^\gamma + \delta^2(z' - \xi') = 1. \tag{12}$$

The non-dimensional parameters that characterise the motion are the ratio of specific heats γ, the buoyancy parameter

$$\delta = (\rho_w g R_m/p_\infty)^{1/2}, \tag{13}$$

and the strength parameter

$$\alpha = p_0/p_\infty. \tag{14}$$

As a buoyant bubble collapses in an infinite fluid its added mass falls and it accelerates upwards. This acceleration causes a local pressure maximum to develop behind the bubble and this drives the motion of the bubble surface here and causes formation of a liquid jet that travels through the bubble. At a given value of the strength parameter, for small buoyancy parameters only part of the jet may be formed when the bubble achieves minimum volume. As the bubble re-expands the jet usually continues to travel through the bubble (Best & Kucera 1992). For larger values of the buoyancy parameter the jet may completely penetrate the bubble prior to it achieving minimum volume. For a given buoyancy parameter similar behaviour is observed as the strength parameter is varied (Best 1991). For small strength parameters the jet does not completely penetrate the bubble prior to minimum volume. As it is increased jet formation occurs earlier and the jet ultimately penetrates the bubble completely before minimum volume is reached. When the jet impacts upon the far side of the bubble it evolves into toroidal form, with an attached vortex ring. The boundary integral method has been extended by Best (1993, 1994) to describe the motion of toroidal bubbles.

To proceed beyond impact, Best connects the jet tip to the other side of the bubble over a small surface which forms a cut across which the potential is discontinuous by $\Delta\phi$. Best (1993) has shown that in an axisymmetric geometry

$$\Delta\phi = \phi_+ - \phi_-, \tag{15}$$

where ϕ_+ and ϕ_- respectively refer to the potential evaluated at the upper and lower impact surfaces just before jet impact. Insertion of the cut allows the flow domain to be considered singly connected and (5) used, with special account taken of the cut geometry. In such a geometry the boundary integral expression for the potential becomes

$$c(\boldsymbol{p})\phi(\boldsymbol{p}) = \int_{\partial\Omega} \left(\frac{\partial\phi}{\partial n}(\boldsymbol{q}) G(\boldsymbol{p},\boldsymbol{q}) - \phi(\boldsymbol{q}) \frac{\partial G}{\partial n}(\boldsymbol{p},\boldsymbol{q}) \right) dS(\boldsymbol{q}) - \Delta\phi \int_T \frac{\partial G}{\partial n_+}(\boldsymbol{p},\boldsymbol{q}) dS(\boldsymbol{q}), \tag{16}$$

where T denotes the cut surface and the subscript $+$ denotes evaluation on its upper surface. In Best's original algorithm the surface T was advected with the fluid. In a later refinement (Best 1994) the surface T is continuously deformed so that its geometry is particularly simple. Recently, toroidal bubble shapes computed using Best's methodology have been favourably compared with experimental data (Blake, Tomita & Tong 1998, Tong, Schiffers, Shaw, Blake & Emmony 1999).

The pressure may be calculated anywhere in the flow field using the Bernoulli equation (7). The potential at and around a point is calculated using (5) or (16) and these values enable accurate computation of the time and space derivatives appearing in (7) using simple finite difference approximations.

Determination of the boundary integral parameters α and δ necessitates knowledge of the initial pressure p_0 and maximum bubble radius R_m. The initial pressure may be determined from assumption of the form (1) for the variation of the bubble pressure and the assumption that the bubble is initially spherical and at rest. Further, the distance scale R_m is the maximum radius to which the bubble would expand in the absence of perturbing effects, that is in the event that the bubble remained spherical. Thus to determine α and δ in terms of the physical parameters γ, ϵ and κ, the motion of a spherical bubble must be considered.

4 The spherical bubble model

Suppose that a bubble undergoes purely radial oscillations at depth ξ. The radius of the bubble is given by the time dependent function R. Supposing that the origin is at the centre of the bubble the velocity potential for radial oscillation is

$$\phi = -R^2\dot{R}/|\boldsymbol{r}|, \tag{17}$$

where the dot denotes differentiation with respect to time and $\boldsymbol{r}$ is the position vector of some point in the flow field.

The usual way to proceed to an equation of motion is via energy conservation. The fluid kinetic energy, T, is obtained as

$$T = \frac{1}{2}\rho_w \int_{\bar{V}} |\nabla\phi|^2 \, d\bar{V} = 2\pi\rho_w R^3\dot{R}^2, \tag{18}$$

where $\bar{V}$ denotes the volume occupied by the fluid. The potential energy of the bubble is equal to the work done in expanding to radius R from zero radius against the hydrostatic pressure and is equal to

$$\mathcal{V} = \frac{4}{3}\pi R^3 p_\infty. \tag{19}$$

The internal energy of the bubble contents is equal to the work done in compressing this gas from zero pressure, or infinite volume, to the bubble volume adiabatically. Hence it is equal to

$$U = -\int_\infty^V p\, dV, \tag{20}$$

where $V = 4\pi R^3/3$ is the bubble volume. If w denotes the mass of explosive, considered equal to the mass of the detonation gas, then from (1) the pressure along an adiabatic characterised by κ is

$$p = \kappa(w/V)^\gamma, \tag{21}$$

so

$$U = \left(\frac{4}{3}\pi\right)^{1-\gamma} \frac{\kappa w^\gamma}{\gamma - 1} R^{3(1-\gamma)}. \tag{22}$$

In consideration of (21) it is pertinent to note that photographic records of underwater explosions suggest that not all the explosive mass is converted to gas upon detonation. The photographs show what appear to be solid remnants of the detonation, which sometimes obscure the image of the bubble surface. It may therefore be appropriate to assume that a fixed proportion of the mass is converted to gas. This would cause the appearance of an additional constant within (21). However, this constant may simply be incorporated into a redefined value of κ and the analysis that follows is unchanged. Given the assumptions made in modelling the water and explosion contents it would be inconsistent to assume that anything but a constant proportion of the explosive mass were converted to gas upon detonation.

The equation of motion is obtained by equating the sum of these energies to the total energy in the bubble oscillation, which is equal to ϵw. To simplify proceedings, appropriate time and length scales are introduced. The distance scale is

$$R_{sc} = \left(\frac{3\epsilon w}{4\pi p_\infty}\right)^{1/3}, \tag{23}$$

and the time scale is

$$T_{sc} = R_{sc}\left(\frac{3\rho_w}{2p_\infty}\right)^{1/2}. \tag{24}$$

Note that these are different from the scales introduced in the previous section. The equation for the non-dimensional bubble radius r is then

$$r^3\dot{r}^2 + r^3 + \mu r^{-3(\gamma-1)} = 1, \tag{25}$$

where

$$\mu = \frac{\kappa p_\infty^{\gamma-1}}{(\gamma-1)\epsilon^\gamma}. \tag{26}$$

At the maximum and minimum radii, $\dot{r} = 0$, so they are given as the solution of

$$r^3 + \mu r^{-3(\gamma-1)} - 1 = 0. \tag{27}$$

Denoting them as $r_{\max}$ and $r_{\min}$ they are given approximately when $\mu \ll 1$ as

$$r_{\min} \approx \mu^{1/(3(\gamma-1))}, \tag{28}$$

and

$$r_{\max} \approx 1 - \mu/3 + (2 - 3\gamma)\mu^2/9. \tag{29}$$

Given these approximate values the solutions may be found numerically using bisection, say.

The solutions of (25) have the characteristic that they are symmetric about the maximum radius. Hence the non-dimensional period of oscillation is given by

$$\tau = 2\int_{r_{\min}}^{r_{\max}} \frac{r^{3/2}}{(1 - r^3 - \mu r^{-3(\gamma-1)})^{1/2}}\, dr. \tag{30}$$

Evaluation of (30) is performed numerically, using Gaussian quadrature, with the singularities in the integrand at both ends of the integration range subtracted and integrated analytically. In the limiting case $\mu = 0$, the integral may be evaluated analytically in terms of the Gamma function and yields $\tau = \sqrt{3/\pi}\,\Gamma(5/6)\Gamma(2/3) = 1.4937$.

For future reference it is worthwhile to write down expressions for the maximum and minimum radii and the oscillation period. The period is

$$T = \left(\frac{3}{2g}\right)^{5/6}\left(\frac{\epsilon}{2\pi\rho_w}\right)^{1/3}\frac{w^{1/3}}{(\xi + \xi_0)^{5/6}}\,\tau, \tag{31}$$

the maximum radius is

$$R_m = \left(\frac{3\epsilon}{4\pi\rho_w g}\right)^{1/3}\left(\frac{w}{\xi + \xi_0}\right)^{1/3} r_{\max}, \tag{32}$$

and the minimum radius is

$$R_0 = \left(\frac{3\epsilon}{4\pi\rho_w g}\right)^{1/3}\left(\frac{w}{\xi + \xi_0}\right)^{1/3} r_{\min}. \tag{33}$$

Using the minimum radius, p_0 may be evaluated from (1) and the strength parameter α is given in terms of the explosive charge parameters by.

$$\alpha = \kappa p_\infty^{\gamma-1}/(\epsilon r_{\min}^3)^\gamma = (\gamma - 1)\mu/r_{\min}^{3\gamma}. \tag{34}$$

The buoyancy parameter is

$$\delta = (\rho_w g R_m/p_\infty)^{1/2} = (R_m/(\xi + \xi_0))^{1/2}. \tag{35}$$

For later comparison an expression is required for the pressure experienced in the fluid at bubble minimum. In dimensional variables, the pressure is given by the Bernoulli equation (7) as

$$p_w/\rho_w = p_\infty/\rho_w - \frac{\partial\phi}{\partial t} - \frac{1}{2}|\nabla\phi|^2, \tag{36}$$

noting that the term involving the gravitational acceleration is not consistent with the spherical bubble assumption. From (17) it follows that

$$\frac{\partial \phi}{\partial t} = -(2R\dot{R}^3 + R^2\ddot{R})/|\boldsymbol{r}|, \tag{37}$$

and

$$|\nabla\phi|^2 = R^4\dot{R}^2/|\boldsymbol{r}|^4. \tag{38}$$

The maximum pressure occurs at bubble minimum when $\dot{R} = 0$ so

$$p_{\max}(\boldsymbol{r})/p_\infty - 1 = \frac{2}{3}\frac{r_{\min}^2\ddot{r}_{\min}}{|\boldsymbol{r}|}, \tag{39}$$

where the distance and time scales (23) and (24) have been used and $\ddot{r}_{\min}$ is the second time derivative of the non-dimensional radius at minimum volume. Differentiating (25) with respect to time, dividing through by $\dot{r}$ and then setting it equal to zero yields

$$\frac{2}{3}\frac{r_{\min}^2\ddot{r}_{\min}}{|\boldsymbol{r}|} = r_{\min}((\gamma-1)\mu r_{\min}^{-3\gamma} - 1), \tag{40}$$

where (27) has been used. Noting the definition of the strength parameter α in (34), the peak pressure at bubble minimum may be written as

$$p_{\max}(\boldsymbol{r})/p_\infty - 1 = (\alpha - 1)r_{\min}/|\boldsymbol{r}|. \tag{41}$$

Note that in this expression $|\boldsymbol{r}|$ is non-dimensional with respect to $R_{\rm sc}$.

5 Determination of the parameters

The first point to be made with respect to a determination of the three bubble parameters γ, ϵ and κ following the technique of Arons (1948) is that only two pieces of information, namely equation (2) and peak pressure data are available. Thus the strategy to be followed is to determine the three parameters so that the theoretical bubble period differs, in a least squares sense, from (2) by as little as possible, and that the peak pressure at bubble minimum is in agreement with the experimental data. The essential difference between this work and that of Arons is that here the restrictive spherical bubble assumption is removed through use of the boundary integral method to compute the bubble motion and peak pressure.

That the bubble period data, as opposed to maximum radius data, should be central to any determination of the bubble parameters stems from the fact that this characteristic of the explosion event may be easily measured from a pressure record. Data for the maximum bubble radius requires that high speed photography be employed in such a manner that reliable distance measurements may be undertaken. In addition, it is often found in high speed photography of underwater explosion events that the bubble surface is not smooth, a feature that introduces error into determinations of the maximum radius.

Before embarking on the computations it is noted that deformation of the bubble from spherical shape does not affect the bubble period by an amount that is significant in the

context of these calculations. *A posteriori* calculations show that for a charge of mass 5.448 kg over the range of depths from 10 m - 150 m, the period as computed using the boundary integral method differs from the spherical bubble value by at most 0.67%. For depths of 50 m and below the deviation is at most 0.15%. This deviation is negligible given uncertainty in the experimental data. Hence the spherical bubble expression for the period is used.

To proceed, compare the expressions of (2) and (31). It is assumed that the three bubble parameters are constants and not dependent upon the charge mass or depth of detonation. In this event, equating (2) and (31) indicates that the non-dimensional bubble period τ is constant. It is clear from (30) that τ is dependent upon depth via its dependence upon μ. Consider figure 1, which displays the non-dimensional bubble period as a function of μ for different values of γ. This figure has been generated following Swift & Decius (1947) and Arons (1948). Values of μ that are realised in practice generally range over the interval $(0, 0.4)$, a fact that is confirmed *a posteriori*, once the parameters have been estimated. Arons used such a figure to select a value of γ such that the variation of the non-dimensional period would be minimal, following comparison of (2) and (31). Arons chose a value of 1.25. The value of 5/4 also renders the exponents in (25) and (26) easily simplified.

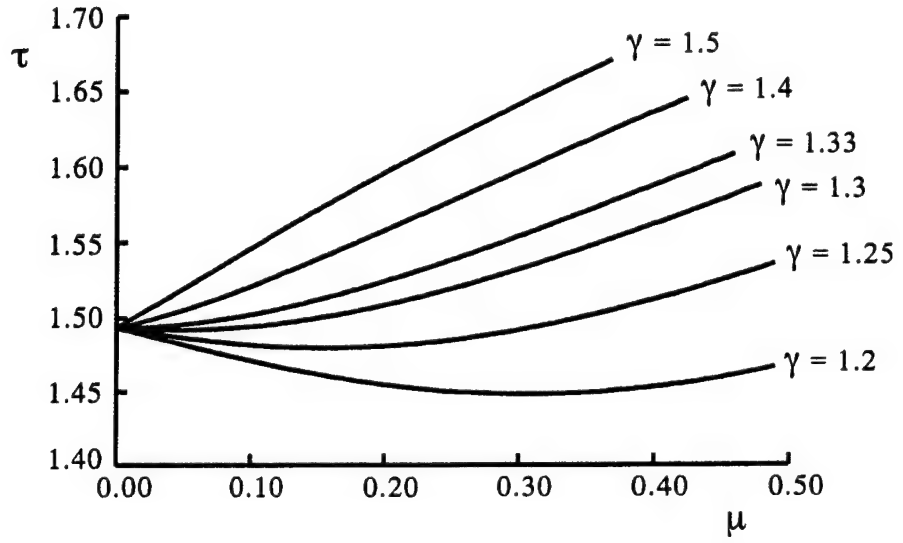

Figure 1: The non-dimensional bubble period τ as a function of μ for a selection of values of γ.

This technique is to be followed here, but with greater precision. It is supposed that (2) is valid over a range of depths, here taken to be 0 - 150 m, in accordance with comments by Arons (1948). Given values for the parameters γ, ϵ and κ, this range can be equivalently considered a range of μ. Suppose it takes on values in the range $(\mu_{\min}, \mu_{\max})$ for some maximum and minimum values. Denote $\Delta\mu = \mu_{\max} - \mu_{\min}$. Over this range the mean

non-dimensional period is

$$\bar{\tau}(\gamma) = \Delta\mu^{-1} \int_{\mu_{\min}}^{\mu_{\max}} \tau(\mu, \gamma)\, d\mu, \tag{42}$$

and the mean square deviation is

$$\begin{aligned} \bar{\Delta\tau^2}(\gamma) &= \Delta\mu^{-1} \int_{\mu_{\min}}^{\mu_{\max}} (\tau(\mu, \gamma) - \bar{\tau}(\gamma))^2\, d\mu, \\ &= \Delta\mu^{-1} \int_{\mu_{\min}}^{\mu_{\max}} \tau^2(\mu, \gamma)\, d\mu - \bar{\tau}^2(\gamma). \end{aligned} \tag{43}$$

The procedure adopted is to find the value of γ such that $\bar{\Delta\tau^2}$ is a minimum. It should be noted that γ is restricted to lie in the regime of physical values for gases, namely $(1, 5/3]$. In the absence of values for γ, ϵ and κ the initial choice for the range $(\mu_{\min}, \mu_{\max})$ is $(0.0, 0.35)$. The integrals of (42) and (43) are evaluated using Gaussian quadrature and the minimum is determined using a golden section search (Press *et al.* 1992).

Denote by $\bar{\tau}$ the mean value of τ at the value of γ determined by minimisation of (43). The bubble energy per mass of explosive is then given by equating (2) and (31) and is

$$\epsilon = 2\pi\rho(2g/3)^{5/2}(K/\bar{\tau})^3. \tag{44}$$

The remaining part of the calculation involves a determination of κ in order to reconcile theoretical predictions of the peak pressure upon bubble rebound with the experimental data of Arons *et al.* (1948). Following estimation of κ, a more reliable estimate of the range of values of μ may be made. The procedure for estimating the three bubble parameters is then repeated to yield refined estimates. Given the accuracy of the experimental data and numerical limitations, the procedure is iterated only once.

It is appropriate to comment that two parameters are essentially determined on the basis of the bubble period data. It must be emphasised that this characteristic of the bubble event is by far the easiest to measure and it is therefore appropriate that it be utilised to maximum extent in determination of the physical parameters that characterise the bubble contents.

To proceed to a determination of κ requires that $p_{\max}(R_p)$ be determined as a function of κ, following estimation of γ and ϵ. Given that a computation of the whole bubble motion using the boundary integral method is required to determine this pressure for each value of κ, the technique used was designed to minimise the number of computations. The required pressure was evaluated for κ equal to 1.0×10^5, 1.125×10^5, 1.25×10^5, 1.375×10^5, 1.5×10^5 and 1.625×10^5, values that were found to well cover the region where the solution was found. A cubic spline was fitted to the data to interpolate a smooth curve and a bisection method used to find the value of κ at which the theoretical prediction of pressure coincided with the experimental data.

In order to provide some estimate of the accuracy of the parameters determined, the procedure was repeated using values for the coefficient K and the peak pressure that are at the extremes of the ranges defined by the error estimates quoted in section 2. Calculating over all combinations of extreme values provides extreme estimates of γ, ϵ and κ and hence estimates of error.

To perform the calculations presented here requires values to be fixed for the fluid density, atmospheric head and gravitational acceleration. These values are taken to be as follows:

$$\begin{aligned} \rho_w &= 1027.6\,\mathrm{kg\,m^{-3}}, \\ \xi_0 &= 10.05\,\mathrm{m}, \\ g &= 9.81\,\mathrm{m\,s^{-2}}. \end{aligned}$$

This value for the fluid density is that of sea water at 5° C. The boundary integral method computes pressures scaled with respect to the hydrostatic pressure at the depth of detonation. With this scaling, the peak pressure recorded by Arons *et al.* (1948) for a charge of mass 5.448 kg at a depth of 152.4 m, quoted in section 2, is equal to 5.842 ± 0.210.

The values obtained for the parameters characterising the bubble contents are:

$$\begin{aligned} \gamma &= 1.23, \\ \epsilon &= (2.08 \pm 0.03) \times 10^6\,\mathrm{J\,kg^{-1}}, \\ \kappa &= (1.46 \pm 0.05) \times 10^5, \end{aligned}$$

noting that to three significant figures γ is errorless.

For comparison, the calculation was also performed using peak pressure data for the 1.137 kg charge detonated at a depth of 76.2 m. The peak over-pressure recorded by Arons *et al.* (1948) was 7.033×10^6 Pa (1020 lb/in^2). The values obtained are: $\gamma = 1.23$, $\epsilon = 2.09 \times 10^6\,\mathrm{J\,kg^{-1}}$, $\kappa = 1.53 \times 10^5$. Only the value for κ is outside the quoted error range, indicating the sensitivity of this parameter to the pressure data.

The values determined above are close to those given by Arons (1948):

$$\gamma = 1.25, \quad \epsilon = 2.05 \times 10^6\,\mathrm{J\,kg^{-1}}, \quad \kappa = 1.45 \times 10^5.$$

That the values for γ and ϵ should be close follows from their determination primarily using period data, in conjunction with the observation that deformation of the bubble from spherical shape during collapse has negligible effect upon the period. Closer investigation of the effect of bubble deformation upon the pressure field surrounding the bubble shows the close agreement of κ to be somewhat fortuitous.

6 Variation of the pressure

Having determined the parameters characterising the bubble contents, it is interesting to compute the pressure field around the bubble, and particularly the maximum value as the bubble rebounds for the first time. The calculations presented here are of the pressure at a distance from the charge that satisfies (4) and these are compared with the spherical bubble expression (41).

First, the pressure has been calculated at a radius satisfying (4), for a range of charge masses between 1 kg and 1000 kg, at a depth of 152.4 m, which replicates the conditions under which the experimental data used here were compiled. The results are shown in

figure 2. The unevenness of this curve arises from effects associated with numerical differentiation used in computation of the pressure. Also shown is the expression obtained from the spherical bubble model. In this model, for a given depth, the pressure is constant for w and R_p satisfying (4). The results obtained using the boundary integral method show significantly more complex behaviour of the peak pressure and this is due to translation and deformation of the bubble from spherical shape.

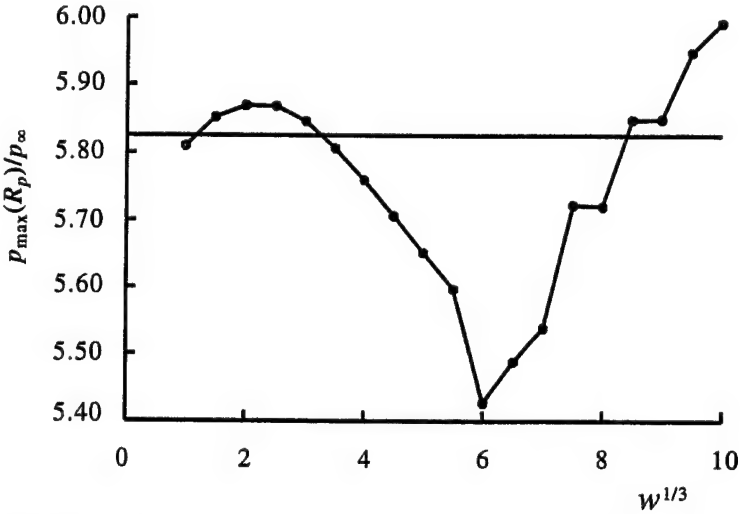

Figure 2: The non-dimensional peak pressure experienced at R_p due to bubble rebound, as a function of $w^{1/3}$. The depth is 154.2 m. The smooth curve is the prediction of the spherical bubble model.

For small charge masses the peak pressure is close to the value predicted by the spherical model. As the charge mass increases the peak pressure falls and reaches a local minimum, after which it begins to increase rapidly. Inspection of the bubble shapes during the collapse and rebound demonstrates features that correlate with these features of the peak pressure and hence assist in interpreting the behaviour. Consider the case where $w^{1/3} = 1.76$, which corresponds to the data presented by Arons *et al.* (1948) and used here. The bubble collapse and rebound are shown in figure 3, the bubble being spherical to a high degree of approximation during the first expansion, which is not shown. The critical observation is that the bubble is close to spherical as it rebounds. A flattening of the lower surface is evident at minimum volume and is a prelude to jet formation upon bubble rebound. As the bubble rebounds the jet develops and travels through the bubble, as first documented by Best & Kucera (1992). Once the jet completely penetrates the bubble, an event referred to as jet impact, it evolves into toroidal form, as shown in figure 4. There is a weak circulation around the torus. As the bubble continues to re-expand the thread of fluid flowing through the torus thins and it appears that the bubble will resume a singly connected topology. Computation of the subsequent behaviour has been given by Best (1994).

Given the degree to which the bubble may be approximated as spherical at the time of rebound, it is no surprise that the boundary integral method and spherical bubble model

are in approximate agreement as to the peak pressure. As the charge mass increases so does the degree of jet formation at bubble minimum. The quantity of fluid kinetic energy at the minimum therefore increases and as a consequence of energy conservation the bubble does not collapse to as small a volume as it would if it remained spherical and stationary. This reasoning is consistent with the evidence of figure 5 which shows the variation with charge mass of the bubble volume at the first minimum. The time derivative of the velocity potential around the time of first minimum is dominated by a term that reflects the rate of change of bubble volume. As the minimum volume increases with charge mass, its time derivative and that of the velocity potential decreases. The non-dimensional peak pressure at R_p therefore decreases with charge mass.

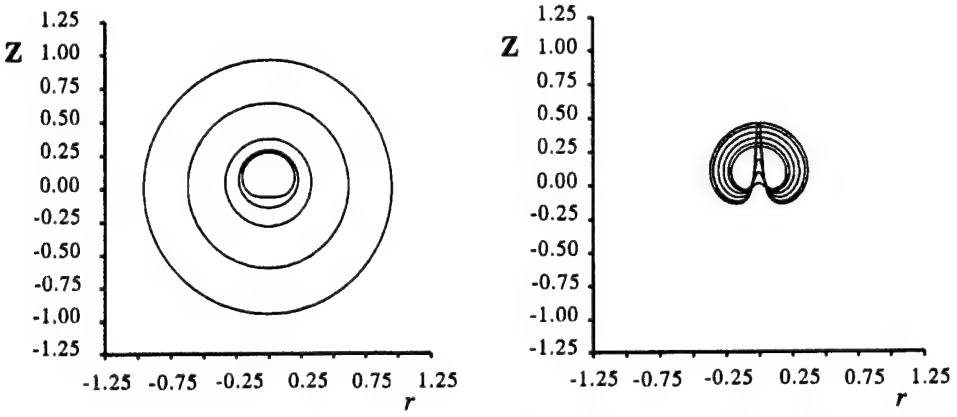

Figure 3: The collapse (a) and rebound (b) of the bubble created by detonating 5.448 kg TNT at a depth of 154.2 m. The distance scale is non-dimensional with respect to the maximum bubble radius, equal to 1.04 m. The times, in milliseconds, corresponding to the bubble shapes are: (a) 34.92, 48.01, 52.06, 52.95, 53.33, (b) 53.58, 53.82, 54.11, 54.43, 54.76, 54.98.

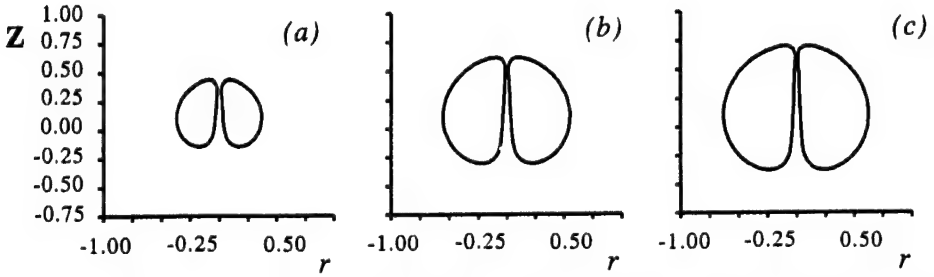

Figure 4: The motion of the toroidal bubble formed during the rebound of the bubble created by detonating 5.448 kg TNT at a depth of 154.2 m. The distance scale is non-dimensional with respect to the maximum bubble radius, equal to 1.04 m. The times, in milliseconds, corresponding to the bubble shapes are: (a) 54.98, (b) 55.70, (c) 56.15.

As the charge mass is increased further the stage is reached where the bubble evolves into toroidal form before minimum volume is reached. An example is illustrated in figures

6 and 7, for the case $w^{1/3} = 7$. Under such circumstances the bubble at minimum volume has an attached vortex ring and the peak pressure in this regime is an increasing function of the charge mass. Notice that the local minimum in the peak pressure curve of figure 2 corresponds closely with that charge mass at which the bubble becomes toroidal at minimum volume. It appears that this extremum in the peak pressure is a signature of this change in physical behaviour from the bubble being singly connected at minimum volume to being a toroidal bubble with an attached vortex ring at this time.

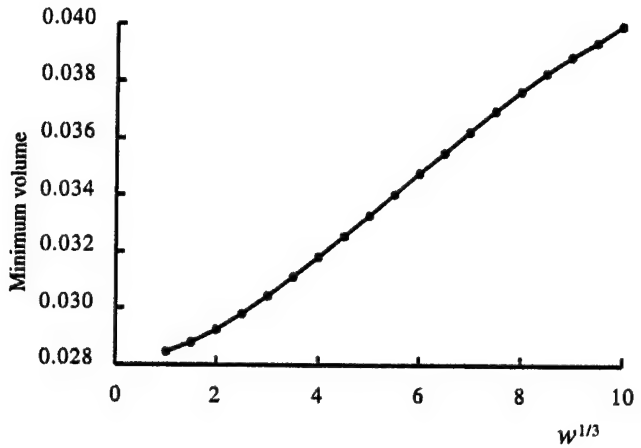

Figure 5: The volume of the bubble at the first minimum, as a function of $w^{1/3}$. The depth of detonation is 154.2 m. The volume is non-dimensional, with the distance scale the maximum bubble radius.

In this context it is worthwhile recalling computations of the pressure field in the fluid before and after toroidal bubble formation as presented by Best (1993). These demonstrate that before jet impact there is a local maximum in the pressure field located behind the bubble and driving the jet through it. After jet impact the location of this local maximum changes to a position ahead of the bubble and the value of the maximum is enhanced. The action of the peak pressure here is to decelerate the rush of fluid through the torus and drive the circulatory motion of fluid around the torus. The local minimum in the peak pressure as a function of charge mass noted in figure 2 clearly reflects the change in character of the pressure field brought about by toroidal bubble formation. For smaller charge masses the peak pressure at rebound reflects the pressure field associated with a singly connected bubble that exhibits a local maximum behind the bubble. For larger charge masses the peak pressure at bubble rebound reflects the pressure field associated with a toroidal bubble that exhibits a local maximum ahead of the bubble.

It is instructive to interpret the changing behaviour of the bubble with charge mass in terms of the non-dimensional parameters introduced in conjunction with the boundary integral method. The strength parameter α is independent of charge mass, so plays no role in interpretation of the present set of results. The key parameter is the buoyancy parameter, given by (35). At a given depth δ varies as $w^{1/6}$. The variation of bubble behaviour with buoyancy parameter has been systematically investigated by Best & Kucera

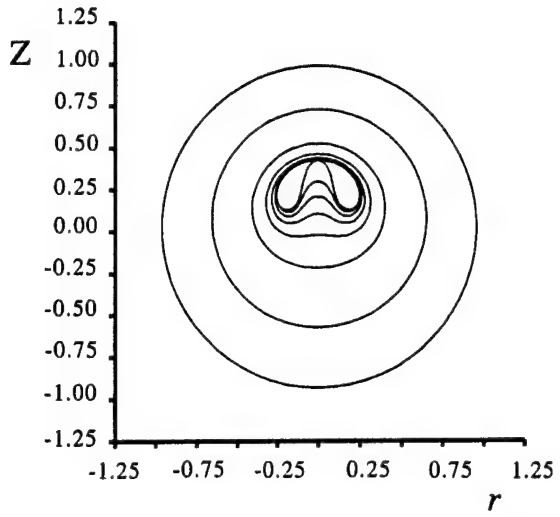

Figure 6: The collapse of the bubble created by detonating 343 kg TNT at a depth of 154.2 m. The distance scale is non-dimensional with respect to the maximum bubble radius, equal to 4.13 m. The times, in milliseconds, corresponding to the bubble shapes are: 136.6, 188.0, 204.7, 208.5, 210.1, 211.1, 211.9, 213.1.

(1992). The key role that buoyancy plays in the jet formation process is to cause the rapid acceleration upwards of the approximately spherical bubble as it begins to collapse. The consequence of this is development of a localised pressure maximum behind the bubble which drives the jet through the bubble.

As the buoyancy force, as quantified by δ, increases, jet formation occurs earlier. For small charge masses this causes more energy to manifest itself in the form of fluid kinetic energy at the time of minimum volume, causing an increase in the minimum volume and consequent downward trend in peak pressure. As the buoyancy parameter increases further a stage is reached where jet penetration coincides with the bubble minimum. As δ increases further jet penetration occurs earlier and rebound occurs after the bubble has evolved into toroidal form. In this regime, the fluid motion associated with the circulation around the torus causes the peak pressure to increase with δ.

An additional set of calculations has been performed for the maximum pressure at R_p due to bubble rebound in the case where the depth is 76.2 m, which corresponds to the other depth at which Arons *et al.* (1948) gathered pressure data. The maximum pressure as a function of charge mass is shown in figure 8. This figure also displays the value given by the spherical bubble model as the constant curve. There are two aspects to note when comparing this figure to figure 2, which corresponds to a depth of 152.4 m. The strength parameter α is greater at the smaller depth and for a given charge mass the buoyancy parameter varies as $(\xi + \xi_0)^{-2/3}$, to leading order. Hence a smaller depth yields a larger buoyancy parameter. This is in accordance with the observation that a given mass of explosive will form a larger bubble at smaller depth owing to the reduced hydrostatic pressure, with the buoyancy force consequently larger.

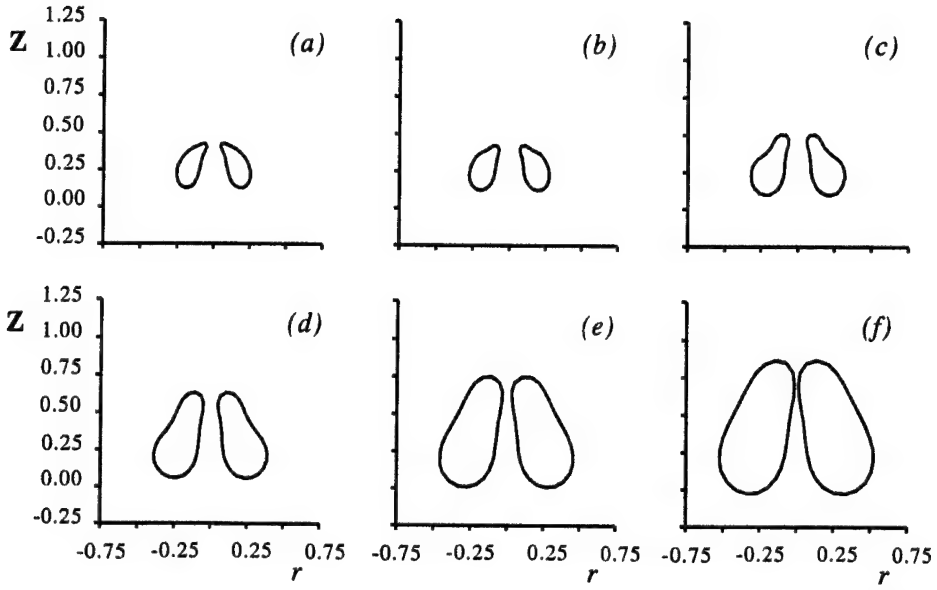

Figure 7: The motion of the toroidal bubble formed following collapse of the bubble created by detonating 343 kg TNT at a depth of 154.2 m. The distance scale is non-dimensional with respect to the maximum bubble radius, equal to 4.13 m. The times, in milliseconds, corresponding to the bubble shapes are: (a) 213.1, (b) 214.2, (c) 215.9, (d) 218.6, (e) 222.2, (f) 226.6.

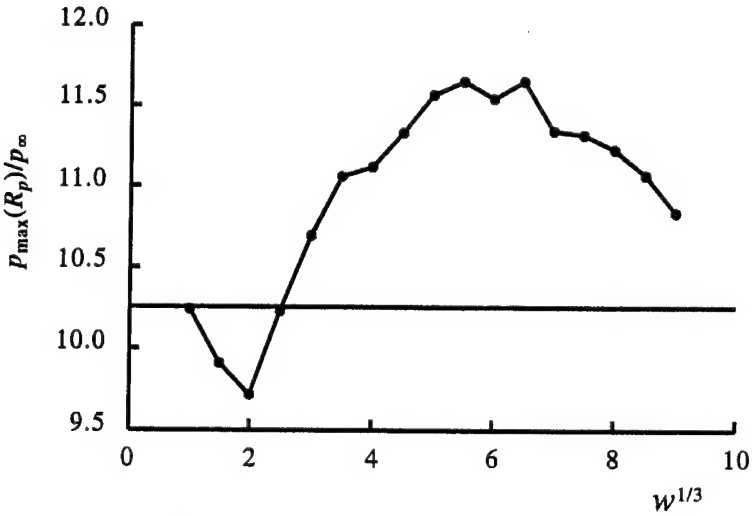

Figure 8: The non-dimensional peak pressure experienced at R_p due to bubble rebound, as a function of $w^{1/3}$. The depth is 76.2 m. The smooth curve is the prediction of the spherical bubble model.

In this example, the bubble for which $w^{1/3} = 1.5$ reached minimum volume just prior to the transition to a toroidal geometry, and for $w^{1/3} = 2.0$ the bubble became toroidal just prior to achieving minimum volume. Hence the local minimum of the peak pressure curve again corresponds with the coincidence of jet impact and minimum volume. That this correspondence should occur at a much smaller charge mass is due to the two effects noted above for the strength parameter and buoyancy parameter. The strength parameter provides some measure of the rate of change of bubble volume, and hence added mass, as the bubble collapses. The greater the rate of change the larger the upwards acceleration of the bubble. The increased buoyancy parameter acts similarly, causing earlier jet formation. The additional feature evident from these data, compared with those of figure 2, is the behaviour of the maximum pressure as the charge mass is increased. Once the bubble becomes toroidal before minimum volume is reached, the peak pressure at R_p increases with w. However, a maximum is achieved and thereafter it falls.

A final series of computations was performed to explore the variation of peak pressure at R_p for a given charge mass, as the depth varies. The data are shown in figure 9 for $w = 3.375$ kg. The pressure scale here is atmospheric pressure. Also shown is the value predicted by the spherical model, which displays a monotonic increase with depth. At the larger depths the two results are in close agreement. This reflects the fact that both the strength and buoyancy parameters decrease with depth and the bubble therefore is approximately spherical at the time of the first minimum. As the depth decreases, both increase and cause jet formation to occur earlier. The coincidence of the transition from simply connected to toroidal geometry and minimum volume occurs at a depth between 70 m and 65 m, and this corresponds to a local minimum of the peak pressure variation. As the depth decreases towards this extremum, the greater extent of jet formation at minimum volume results in increased fluid kinetic energy at the expense of bubble internal energy and hence the minimum volume increases. The peak pressure is thus below the spherical bubble prediction. As the bubble becomes toroidal at minimum volume the nature of the flow field manifests itself as an increasing peak pressure. As the parameters α and δ that quantify jet formation increase further with decreasing depth the peak pressure reaches a maximum and thereafter decreases. This trend is as noted in figure 8.

To obtain further insight into the factors affecting the variation of peak pressure with depth, it is useful to compute the peak pressure caused by bubble rebound in a spherical bubble model in which bubble translation is taken into account. In this case the fluid velocity potential is

$$\phi = -\frac{R^2\dot{R}}{|\boldsymbol{r}-\boldsymbol{z}|} - \frac{R^3 U \boldsymbol{e}_z.(\boldsymbol{r}-\boldsymbol{z})}{2|\boldsymbol{r}-\boldsymbol{z}|^3}, \tag{45}$$

where $\boldsymbol{e}_z$ is a unit vector in the vertical direction, $\boldsymbol{z} = z\boldsymbol{e}_z$ is the position vector of the bubble centroid and $U = \dot{z}$ is the velocity of the bubble. Consideration of energy and momentum conservation yield the following equations of motion (Best 1991):

$$R\ddot{R} + \frac{3}{2}\dot{R}^2 - \frac{1}{4}U^2 = \frac{p_0}{\rho_w}(R_0/R)^{3\gamma} + gz - \frac{p_\infty}{\rho_w}, \tag{46}$$

$$\frac{d}{dt}(R^3 U) = 2gR^3. \tag{47}$$

In these expressions it is assumed that at $t = 0$ the bubble centroid is located at $z = 0$ and the bubble is stationary so $U = 0$. These equations may be solved numerically using

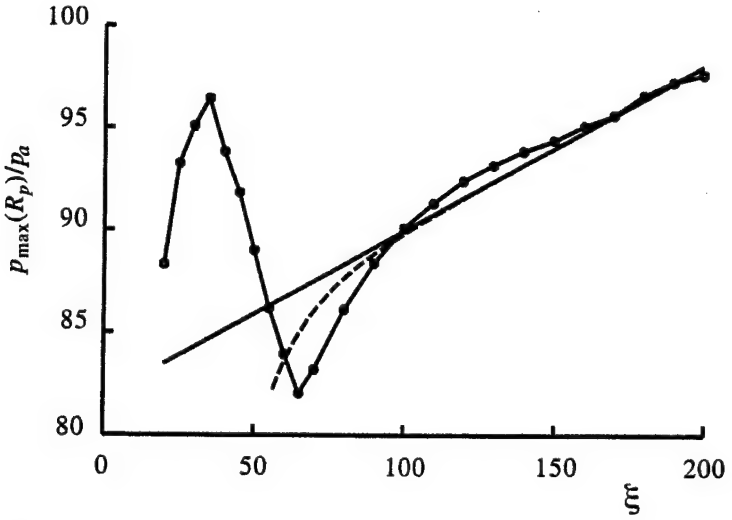

Figure 9: The non-dimensional peak pressure experienced at R_p due to bubble rebound, as a function of detonation depth. The charge mass is 3.375 kg and the pressure scale is atmospheric pressure. The smooth solid curve is the prediction of the stationary spherical bubble model. The dashed curve is the prediction of the translating spherical bubble model.

standard techniques and use of (45) in the Bernoulli equation (7) permits computation of the pressure field in the fluid.

The peak pressure at bubble rebound as a function of depth is shown as the dashed curve in figure 9. Compared with the stationary spherical bubble model, the translating spherical bubble model shows a decrease in the peak pressure as depth decreases. This trend is in accordance with the variation computed using the boundary integral method. At the greater depths, it has been established that the bubble remains spherical at the first minimum, to a high degree of approximation. In this regime the translating spherical bubble model might be expected to well describe the behaviour.

It is instructive to compute the maximum centroid velocity during the first bubble collapse and early rebound phase using both the boundary integral method and the spherical bubble model. The results are shown in figure 10. In this figure the velocity is dimensionless with respect to that computed with the boundary integral method at the maximum depth of 200 m. In this context, note that the velocity scale varies as $(\xi + \xi_0)^{1/2}$, hence the requirement to fix a depth to scale all results.

These results are quite interesting and assist in interpreting the behaviour. They show that, even for quite large depths, when the jet has only partially formed at bubble minimum, the upwards velocity of the non-spherical bubble is noticeably less than the value predicted using the spherical model. In addition, figure 9 shows that the pressure predicted using the boundary integral method and translating spherical bubble model begins to deviate from that predicted using the stationary spherical bubble model at a depth of around 80-100 m. At this depth the translating spherical bubble models predicts an upwards velocity about twice that given by the boundary integral method.

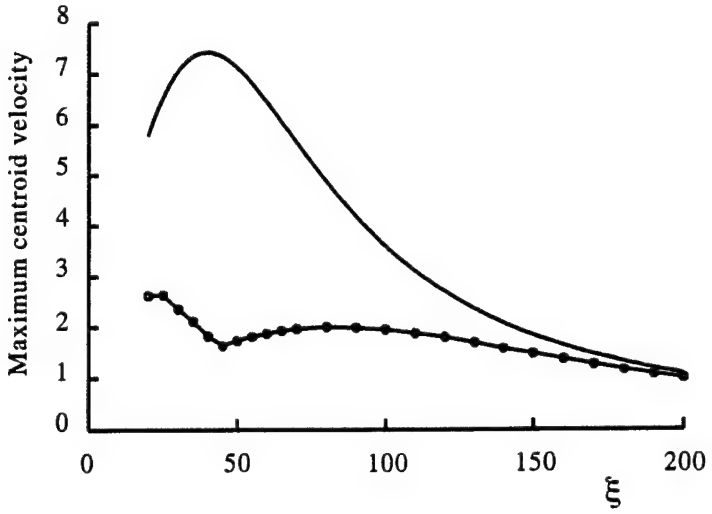

Figure 10: The maximum centroid velocity during the collapse phase, as a function of depth, computed using the boundary integral method. The charge mass is 3.375 kg and the velocity scale is the value predicted at a depth of 200 m. The smooth curve represents computations using the translating spherical bubble model.

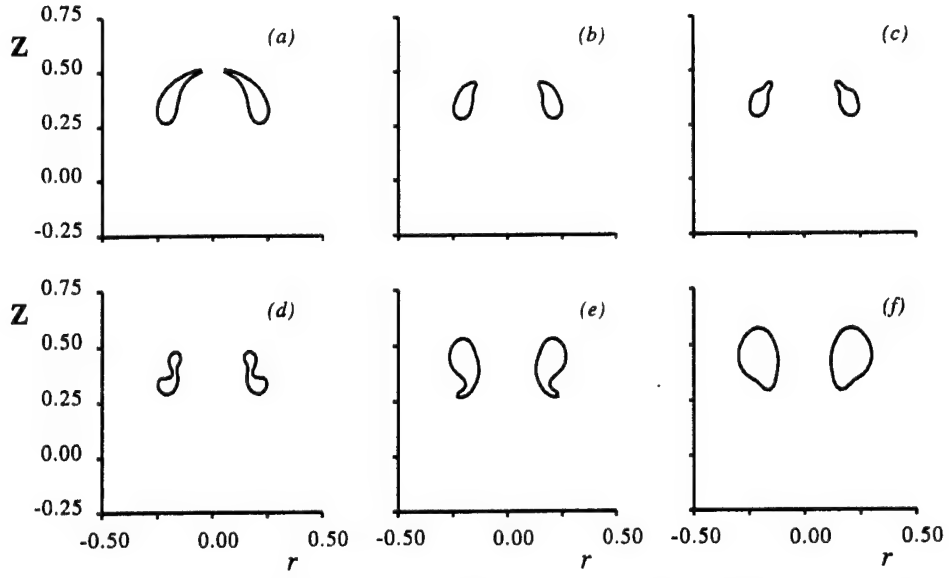

Figure 11: The motion of the toroidal bubble formed following collapse of the bubble created by detonating 3.375 kg TNT at a depth of 20 m. The distance scale is non-dimensional with respect to the maximum bubble radius, equal to 1.64 m. The times, in milliseconds, corresponding to the bubble shapes are: (a) 185.8, (b) 186.1, (c) 186.3, (d) 186.7, (e) 187.6, (f) 188.2.

If the deviation of the pressure from that predicted using the stationary spherical bubble model was due to translation alone then we would expect the centroid velocities given by the boundary integral method and translating spherical bubble model to be similar. The fact that they differ by a factor of about two demonstrates that the deviation of the pressure from the stationary spherical bubble model prediction is not due to translation alone but a combination of translation and deformation from spherical shape.

As the depth decreases further, the translating spherical bubble model predicts a peak pressure that continues to fall, whereas the boundary integral method calculation shows that the pressure has a local minimum at the depth where minimum volume and the transition to a toroidal topology coincide. This divergence in predictions indicates that the variation of peak pressure with depth reflects the complex flow field of the toroidal bubble with attached vortex ring. It also illustrates that in this regime the stationary spherical bubble model is superior to that which includes translation in predicting the pressure in the flow field.

The variation of peak pressure with depth, as computed using the boundary integral method and illustrated in figure 9, shows three distinct regimes, separated by a local maxima and minima. It might be suggested that these correspond to different regimes of bubble behaviour. The discussion above suggests that at large depth values the significant attribute of the bubble behaviour is that jet impact has not occurred prior to bubble rebound. It further suggests that the regime in which maximum pressure increases as depth decreases is characterised by bubble rebound occurring after the bubble has evolved into toroidal form. It is therefore instructive to inspect the bubble shapes for a depth in the regime where the bubble is toroidal at minimum volume but the peak pressure is decreasing with decreasing depth in order to identify any possible behaviour that may characterise this regime. The motion of the toroidal bubble at a depth of 20 m is shown in figure 11. After jet impact the bubble continues to collapse and a depression in the bubble shape is formed and swept around the bubble by the circulation. As the bubble begins to re-expand the depression vanishes. It might be supposed that in some circumstances this depression would pinch the bubble off in the middle and form two counter-rotating toroidal bubbles. This pronounced depression may be a signature of this regime where peak pressure decreases as the depth decreases. It is noted that the formation of such deep depressions in the bubble shape following transition to a toroidal geometry is evident in computations of transient bubble collapse near a rigid boundary (Tong *et al.* 1999). In these cases the boundary induces asymmetry in the flow field and causes jet formation, rather than gravity as in this case.

7 Discussion

In this report the technique of Arons (1948) for determining the parameters that characterise the adiabatic model of underwater explosion bubble contents has been revised to take account of the effect of non-spherical bubble collapse. The technique has also been amended to provide increased accuracy with respect to the deviation between theoretical and experimental values of the period.

The parameters predicted are close to those originally given by Arons (1948), but

investigation of the effect of non-spherical collapse on the pressure field suggests that the agreement is somewhat fortuitous. The boundary integral method has shown significant deviation in the maximum pressure at rebound brought about by translation, non-spherical collapse and toroidal bubble formation. It has been shown that the variation of the peak pressure with depth or charge mass exhibits a distinct local minimum at the point where the transition to a toroidal bubble coincides with the bubble minimum. It has further been shown that if the charge mass and depth are such that only weak oscillation of the bubble occurs then jet formation is suppressed and the spherical model predictions of the pressure are close to those provided by the boundary integral method.

As it happens, the charge masses and depths used by Arons *et al.* (1948) to compile their peak pressure data are in the regime where the bubble is approximately spherical at minimum volume. The formation of liquid jets upon bubble collapse and the transition to a toroidal form were not fully understood at that time. Arons *et al.* (1948) remark that the "twelve-pound charge is the largest that could be tolerated at a distance of 500 ft below the vessel performing the experiments ...". An unforeseen consequence of this practical experimental limitation is that Arons' (1948) original analysis is essentially correct, despite the more complex collapse behaviour of the bubble and pressure field variation documented in this report.

In performing the work reported herein, a number of additional points have come to light concerning various bubble parameters. As noted in the text, the effect of deformation from spherical shape was determined to have virtually no effect on the bubble period. This was established by performing a series of calculations for the 5.448 kg charge over the range of depths 10-150 m. This is equivalent to performing calculations over a substantial region of the α, δ parameter space. These same calculations additionally established the extent to which a buoyant bubble remains spherical through the first expansion. The maximum bubble radius was computed in four ways: as half the maximum horizontal and vertical extents of the bubble and based on the maximum volume and cross sectional area of the bubble. The values determined deviated from a non-dimensional value of 1 by at most 0.15%.

During early phases of this work, attempts were made to determine the bubble parameters using period data and the maximum radius data of (3). A typical approach might be to determine γ and ϵ as done here and then fix κ so that the deviation between theoretical and experimental expressions for the maximum radius is minimised. This methodology is not very satisfactory for a number of reasons. First, the theoretical expression for the maximum radius shows a systematic trend with depth that is not evident in the expression of (3), after the dependence upon $(\xi+\xi_0)^{-1/3}$ is accounted for. Second, as noted in section 2, there is disagreement as to the coefficient J that appears in (3). The variation of this value causes large discrepancies in the values of κ that are determined and this impacts upon predictions of loading significantly.

Consideration of the difficulties involved in compiling data for the maximum radius indicates that these data are probably not as reliable for use in determining the bubble parameters as period and peak pressure data. Explosion bubbles are typically characterised by a surface distorted by phase changes and detonation products. Hence it is difficult to precisely determine the maximum radius. Additionally, it is difficult to deploy the requisite high speed photography in large field trials.

As with all theoretical studies it is appropriate that experimental work be performed in order to assess the validity of the conclusions drawn here. There remains a requirement for decisive experimental data concerning the loads experienced at boundaries due to nearby bubble collapse and jet impact. Once these data are available it would be appropriate to compare the results with computations using the boundary integral method and the parameters given in this report. Such an exercise would provide valuable evidence with which to assess the practical utility of the work reported here.

Final comment concerns the error estimates for the explosion bubble parameters, provided here for the first time. A conservative approach to determining these has been adopted for three reasons. The data of Arons *et al.* (1948) show a reasonable degree of scatter for the peak pressure. Second, the numerical algorithm used for the non-spherical bubble calculations exhibits a small degree of variation as the various numerical parameters that characterise it are varied. Finally, this work has neglected fluid compressibility. Arons *et al.* (1948) measured the pressure at around two maximum radii. It is not unreasonable to suppose that the amplitude of the peak pressure may be modified by compressibility compared with those values predicted here using an incompressible model. The effect of compressibility is to slightly mitigate the pressure so that if the fluid were incompressible the pressures would be higher than those measured. It is supposed that the generous error bounds used here for the peak pressure cover a sufficient range to account for this effect. The error bounds provided here for γ, ϵ and κ are thus considered reliable, especially in the context of predicting loads to structures caused by nearby underwater explosion bubble collapse.

References

1. Abramowitz, M. & Stegun, I. A. (1965) *Handbook of Mathematical Functions,* Dover.

2. Arons, A.B., Slifko, J.P. & Carter, A. (1948) Secondary pressure pulses due to gas globe oscillation in underwater explosions. I. Experimental data. *J. Acoust. Soc. Am.,* **20**, 271-276.

3. Arons, A.B. (1948) Secondary pressure pulses due to gas globe oscillation in underwater explosions. II. Selection of adiabatic parameters in the theory of oscillation. *J. Acoust. Soc. Am.,* **20**, 277-282.

4. Benjamin, T.B. & Ellis, A.T. (1966) The collapse of cavitation bubbles and the pressures thereby produced against solid boundaries. *Phil. Trans. R. Soc. Lond. A,* **260**, 221-240.

5. Best, J.P. (1991) *The dynamics of underwater explosions,* PhD Thesis, University of Wollongong, Australia.

6. Best, J.P. (1993) The formation of toroidal bubbles upon the collapse of transient cavities. *J. Fluid Mech.,* **251**, 79-107.

7. Best, J.P. (1994) The rebound of toroidal bubbles. *Proc. IUTAM Symposium on Bubble Dynamics and Interface Phenomena,* (eds. J.R. Blake, J.M. Boulton-Stone& N.H. Thomas) Kluwer Academic Publishers, 405-412.

8. Best, J.P. & Kucera, A. (1992) A numerical investigation of non-spherical rebounding bubbles. *J. Fluid Mech.,* **245**, 137-154.

9. Blake, J.R. & Gibson, D.C. (1987) Cavitation bubbles near boundaries. *Ann. Rev. Fluid Mech.,* **19**, 99-123.

10. Blake, J.R., Taib, B.B. & Doherty, G. (1986) Transient cavities near boundaries. Part 1. Rigid boundary. *J. Fluid Mech.,* **170**, 479-497.

11. Blake, J.R., Tomita, Y. & Tong, R.P. (1998) The art, craft and science of modelling jet impact in a collapsing cavitation bubble. *Applied Scientific Research,* **58**, 77-90.

12. Chahine, G.L. & Perdue, T.O. (1988) Simulation of the three-dimensional behaviour of an unsteady large bubble near a structure. In *Proc. 3rd Int. Colloq. on Bubbles and Drops,* Monterey, California.

13. Guerri, L., Lucca, G. & Prosperetti, A. (1981) A numerical method for the dynamics of non-spherical cavitation bubbles. In *Proc. 2nd Int. Colloq. on Drops and Bubbles,* JPL Publication 82-7, Monterey, California, 175-181.

14. Lauterborn, W. & Bolle, H. (1975) Experimental investigations of cavitation bubble collapse in the neighbourhood of a solid boundary. *J. Fluid Mech.,* **72**, 391-399.

15. Plesset, M.S. & Chapman, R.B. (1971) Collapse of an initially spherical vapour cavity in the neighbourhood of a solid boundary. *J. Fluid Mech.,* **47**, 283-290.

16. Press, W.H., Teukolsky, S.A., Vetterling, W.T. & Flannery, B.P. (1992) *Numerical recipes in FORTRAN,* Cambridge University Press.

17. Swift, E. & Decius, J.C. (1947) Measurement of bubble pulse phenomena. III. Radius and period studies. In *Underwater Explosion Research,* Vol. II, Office of Naval Research, Washington D.C. (1950) (Eds. G.K. Hartmann & E.G. Hill).

18. Swisdak, M.M. (1978) Explosion effects and properties: II - Explosion effects in water. Naval Surface Warfare Center Report NSWC/WOL TR 76-116.

19. Szymczak, W.G., Rogers, J.C.W., Solomon, J.M. & Berger, A.E. (1993) A numerical algorithm for hydrodynamic free boundary problems. *J. Comput. Phys.,* **106**, 319-336.

20. Szymczak, W.G. & Solomon, J.M. (1996) Computations and experiments of shallow depth explosion plumes. Naval Surface Warfare Center Report NSWCDD/TR-94/156.

21. Tomita, Y. & Shima, A. (1986) Mechanisms of impulsive pressure generation and damage pit formation by bubble collapse. *J. Fluid Mech.,* **169**, 535-564

22. Tong, R.P., Schiffers, W.P., Shaw, S.J., Blake, J.R. & Emmony, D.C. (1999) The role of 'splashing' in the collapse of a laser-generated cavity near a rigid boundary. *J. Fluid Mech.,* **380**, 339-361.

23. Vogel, A., Lauterborn, W. & Timm, R. (1989) Optical and acoustic investigations of the dynamics of laser-produced cavitation bubbles near a solid boundary. *J. Fluid Mech.,* **206**, 299-338.

24. Wilkerson, S. (1989) Boundary integral technique for explosion bubble collapse analysis. *ASME Energy-Sources Techn. Conference and Exhibition,* Houston, Texas.

DISTRIBUTION LIST

The Effect of Non-spherical Collapse on Determination of Explosion Bubble Parameters

John P. Best

	Number of Copies
DEFENCE ORGANISATION	
Task Sponsor	
COMAUSNAVMCDGRP	1
S&T Program	
Chief Defence Scientist	1
FAS Science Policy	
AS Science Corporate Management	
Director General Science Policy Development	
Counsellor, Defence Science, London	Doc Data Sht
Counsellor, Defence Science, Washington	Doc Data Sht
Scientific Adviser to MRDC, Thailand	Doc Data Sht
Scientific Adviser Joint	1
Navy Scientific Adviser	1
Scientific Adviser, Army	Doc Data Sht
Air Force Scientific Adviser	1
Director Trials	1
Systems Sciences Laboratory	
Chief, Weapons Systems Division	Doc Data Sht
Research Leader, Maritime Weapons Systems	Doc Data Sht
Head, Terminal Effects	1
Mr Tim Clarke (WSD)	1
Dr John P. Best (MOD)	1
DSTO Library and Archives	
Library Edinburgh	2
Australian Archives	1
Capability Systems Staff	
Director General Maritime Development	1
Director General Aerospace Development	Doc Data Sht
Knowledge Staff	
Director General Command, Control, Communications and Computers (DGC4)	Doc Data Sht
Navy	
SO (SCIENCE), COMAUSNAVSURFGRP, NSW	Doc Data Sht

Army

ABCA National Standardisation Officer, Land Warfare Development Sector, Puckapunyal	4

Intelligence Program

DGSTA, Defence Intelligence Organisation	1
Manager, Information Centre, Defence Intelligence Organisation	1

Defence Libraries

Library Manager, DLS-Canberra	1
Library Manager, DLS-Sydney West	Doc Data Sht

UNIVERSITIES AND COLLEGES

Australian Defence Force Academy Library	1
Head of Aerospace and Mechanical Engineering, ADFA	1
Deakin University Library, Serials Section (M List), Geelong, Vic	1
Hargrave Library, Monash University	Doc Data Sht
Librarian, Flinders University	1

OTHER ORGANISATIONS

National Library of Australia	1
NASA (Canberra)	1
AusInfo	1
State Library of South Australia	1

INTERNATIONAL DEFENCE INFORMATION CENTRES

US Defense Technical Information Center	2
UK Defence Research Information Centre	2
Canada Defence Scientific Information Service	1
NZ Defence Information Centre	1

ABSTRACTING AND INFORMATION ORGANISATIONS

Library, Chemical Abstracts Reference Service	1
Engineering Societies Library, US	1
Materials Information, Cambridge Scientific Abstracts, US	1
Documents Librarian, The Center for Research Libraries, US	1

INFORMATION EXCHANGE AGREEMENT PARTNERS

Acquisitions Unit, Science Reference and Information Service, UK	1

Library – Exchange Desk, National Institute of Standards and Technology, US	1
Total number of copies:	40

DEFENCE SCIENCE AND TECHNOLOGY ORGANISATION DOCUMENT CONTROL DATA				1. CAVEAT/PRIVACY MARKING
2. TITLE The Effect of Non-spherical Collapse on Determination of Explosion Bubble Parameters			3. SECURITY CLASSIFICATION Document (U) Title (U) Abstract (U)	
4. AUTHOR John P. Best			5. CORPORATE AUTHOR Systems Sciences Laboratory PO Box 1500 Edinburgh, South Australia, Australia 5111	
6a. DSTO NUMBER DSTO–RR–0238	6b. AR NUMBER AR–012–368		6c. TYPE OF REPORT Research Report	7. DOCUMENT DATE July, 2002
8. FILE NUMBER J9505/19/25	9. TASK NUMBER NAV 00/228	10. SPONSOR COMAUSNAVMCDGRP	11. No OF PAGES 25	12. No OF REFS 24
13. URL OF ELECTRONIC VERSION http://www.dsto.defence.gov.au/corporate/reports/DSTO–RR–0238.pdf			14. RELEASE AUTHORITY Chief, Weapons Systems Division	

15. SECONDARY RELEASE STATEMENT OF THIS DOCUMENT

Approved For Public Release

OVERSEAS ENQUIRIES OUTSIDE STATED LIMITATIONS SHOULD BE REFERRED THROUGH DOCUMENT EXCHANGE, PO BOX 1500, EDINBURGH, SOUTH AUSTRALIA 5111

16. DELIBERATE ANNOUNCEMENT

No Limitations

17. CITATION IN OTHER DOCUMENTS

No Limitations

18. DEFTEST DESCRIPTORS

underwater explosions	explosion bubbles
adiabatic conditions	detonation
boundary integral method	buoyancy
oscillations	toroids

19. ABSTRACT

The technique developed by Arons (1948) for determining the parameters that characterise the adiabatic model of underwater explosion bubble contents is revised to account for the effect of non-spherical collapse. Additional modifications are made to enhance accuracy. The parameters predicted are similar to those given by Arons but consideration of the pressure in the fluid when the bubble rebounds shows the agreement to be somewhat fortuitous. Error bounds for the parameters are given for the first time.